International Journal of Mass Spectrometry 279 (2009) 25–31

Contents lists available at ScienceDirect

International Journal of Mass Spectrometry

journal homepage: www.elsevier.com/locate/ijms

Unimolecular dissociation of aniline molecular ion: A theoretical study

Joong Chul Choe[a,*], Nu Ri Cheong[b], Seung Min Park[b]

[a] Department of Chemistry, Dongguk University, Seoul 100-715, Republic of Korea
[b] Department of Chemistry, Kyung Hee University, Seoul 130-701, Republic of Korea

ARTICLE INFO

Article history:
Received 18 August 2008
Received in revised form
25 September 2008
Accepted 25 September 2008
Available online 8 October 2008

Keywords:
DFT calculation
RRKM calculation
Ring contraction
Ring expansion

ABSTRACT

The potential energy surface (PES) for dissociation of aniline ion was determined using density functional theory molecular orbital calculations at the B3LYP/6-311+G(3df,2p)//B3LYP/6-31G(d) level. On the basis of the PES obtained, kinetic analysis was performed by Rice–Ramsperger–Kassel–Marcus (RRKM) calculations. The RRKM dissociation rate constants agreed well with previous experimental data. The most favorable channel was formation of the cyclopentadiene ion by loss of HNC, occurring through consecutive ring opening and re-closure to a five-membered ring. Loss of H• could compete with the HNC loss at high energy, which occurred by direct cleavage of an N–H bond or through ring expansion.

1. Introduction

The unimolecular dissociation of gaseous aniline molecular ion (**1**) has been studied using several experimental means, including electron ionization (EI) [1] and trapped ion mass spectrometry [2], isotope labeling [1,3], photoelectron–photoion coincidence (PEPICO) [4], multiphoton ionization (MPI) [3,5–8], and collision-induced dissociation (CID) [9] methods. It is known that $C_5H_6^{+\bullet}$ is the main primary fragment ion formed from **1**. In the EI [1] and MPI [6] studies, it was assumed that the product $C_5H_6^{+\bullet}$ ion has a linear structure. Baer and Carney measured the dissociation rates on a microsecond time scale as a function of the internal energy using PEPICO [4]. In the study, the critical energy of formation of $C_5H_6^{+\bullet}$ was estimated through model calculations by statistical Rice–Ramsperger–Kassel–Marcus (RRKM) theory [10]. From a comparison with thermochemical data for several $C_5H_6^{+\bullet}$ isomers including linear isomers, they suggested that the product ion is the cyclopentadiene ion ($CP^{+\bullet}$) and that its neutral counterpart is HCN. A year later, Lifshitz et al. [2] reported that HNC is a more reasonable product by measurement of the appearance energy, which is generally accepted.

Rearrangement mechanisms leading to ring expansion or contraction of aromatic gas phase ions has been an interesting subject in theoretical studies. It is well known that the formation of tropylium ion from toluene molecular ion or its derivatives occurs via ring expansion [11–17]. Recently, it was reported that the ring expansion beginning with a 1,2 shift of an H atom of the methyl group is much more favored than with a 1,3-H shift [18]. On the other hand, it was reported that ring expansions in molecular ions of chlorotoluene [19], phenylsilane [20], and its derivatives [21], occurring by a similar mechanism, do not contribute to their dissociations due to high energy barriers for subsequent dissociation steps. A theoretical mechanism for the formation of $CP^{+\bullet}$ from **1** by loss of HNC or HCN was reported, which occurs through ring contractions beginning with a 1,2 or 1,3 shift of the H atom of the amino group [22]. A similar mechanism was reported for the formation of $CP^{+\bullet}$ from phenol molecular ion [23,24].

In this work, we explored the potential energy surface (PES) for the dissociation of **1** using density functional theory (DFT) calculations. Although it is known that the main primary product ion is $C_5H_6^{+\bullet}$ near the threshold, the formation of $C_6H_6N^+$ by loss of H• can contribute to the dissociation at high energy. In the EI [1], MPI [3,5], and CID [9] experiments, the product $C_6H_6N^+$ ion was observed. Several candidates are possible for its structure, including five-, six-, and seven-membered ring isomers. Thus, we examined the H• loss as well as the HNC loss to find out the most favorable reaction pathways and product structures. We found out a novel pathway to form $CP^{+\bullet}$ + HNC, of which energy was lower than that reported previously [22]. Interestingly, we found that both ring contraction and expansion could play roles in the dissociation of **1**. Kinetic analysis by RRKM model calculations was carried out on the basis of the obtained PES to predict the dissociation rate constants.

* Corresponding author. Fax: +81 2 2268 8204.
E-mail address: jcchoe@dongguk.edu (J.C. Choe).

1387-3806/$ – see front matter © 2008 Elsevier B.V. All rights reserved.
doi:10.1016/j.ijms.2008.09.013

2. Computational methods

The molecular orbital (MO) calculations were performed using the Gaussian 03 suite of programs [25]. Geometry optimizations for the stationary points were carried out at the unrestricted B3LYP level of density functional theory (DFT) using the 6-31G(d) basis set. The transition state (TS) geometries connecting the stationary points were searched and checked by calculating the intrinsic reaction coordinates at the same level. Single point energy calculations were carried out at the B3LYP/6-311+G(3df,2p) level to improve the accuracy of the energies. It has been suggested that the B3LYP/6-311+G(3df,2p)//B3LYP/6-31G(d) calculations gives reliable total and reaction energies at 0 K for organic radical cations within ±6 kJ mol^{-1} [26]. The harmonic frequencies, which were calculated at the B3LYP/6-31G(d) level and scaled down by 0.9806 [27], were used for zero point vibrational energy (ZPVE) corrections. The scale factor 0.9614 [27] was used for the individual vibrational frequencies in the RRKM calculations.

The RRKM expression was used to calculate the rate-energy dependences as follows [10]:

$$k(E) = \frac{\sigma N^{\neq}(E - E_0)}{h\rho(E)}, \quad (1)$$

where E is the reactant internal energy, E_0 the critical energy of the reaction, $N^{\neq}$ the sum of the TS states, ρ the density of the reactant states, and σ the reaction path degeneracy. $N^{\neq}$ and ρ were evaluated by a direct count of the states using the Beyer–Swinehart algorithm [28].

3. Results and discussion

3.1. Reaction pathways

Several pathways were found for the formation of $CP^{+\bullet}$ from **1**. The minimum energy reaction pathway (MERP) to $CP^{+\bullet}$ + HNC begins with a 1,3 shift of an H atom of the amino group to form 5-imidocyclohexa-1,3-diene ion (**2a**) via a four-membered ring TS (Scheme 1 and Fig. 1). By a rotation of the NH group, **2b** can be formed. Then, ring opening occurs by cleavage of a C–C bond to form **3a**. After *cis* to *trans* isomerization of **3a** → **3b**, ring closure occurs to form a five-membered ring isomer **4a**. Finally loss of HNC occurs via an ion-neutral complex **5**. The linear isomer, **3a** or **3b**, can lose HNC to form a linear $C_5H_6^{+\bullet}$ isomer, $CH_2CHCHCHCH^{+\bullet}$. However, its endoergicity (535 kJ mol^{-1}) calculated was much higher than that of formation of $CP^{+\bullet}$ (312 kJ mol^{-1}), indicating that the formation of linear $C_5H_6^{+\bullet}$ isomers would be barely observed.

2a can undergo an "H-ring walk" to form **2c**, **2d**, **2e**, and **2b**. From **2c**, **2d**, or **2e**, ring contraction can occur by a single step without ring opening to form **4a**, **4b** or **4a**, respectively. However, their energy barriers were much higher than that of the ring contraction through ring opening of **2b** (Fig. 2). **4a** and **4b** can lose H$^{\bullet}$ to produce a proto-

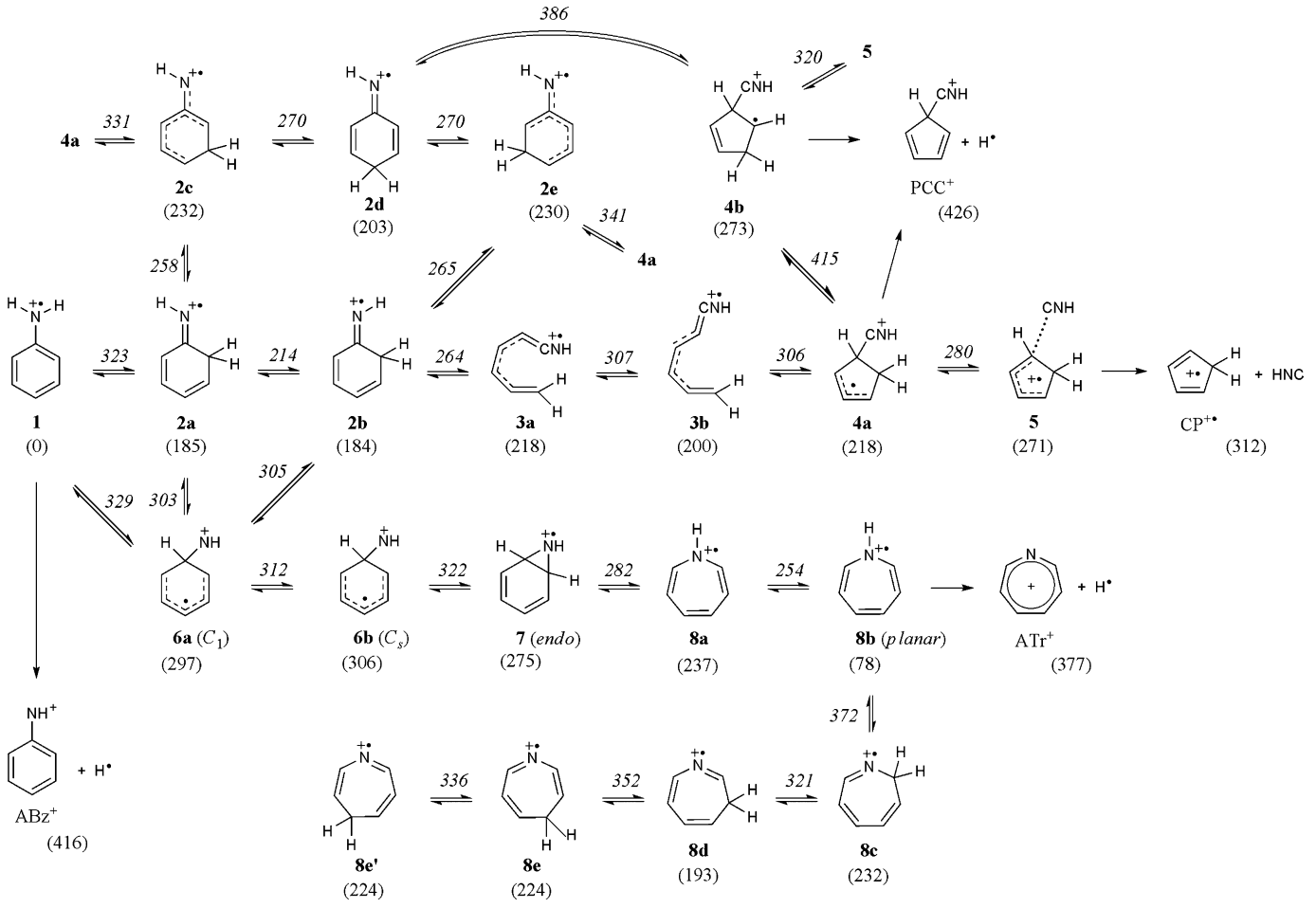

Scheme 1. The isomerization and dissociation pathways of aniline molecular ion obtained from the B3LYP/6-311+G(3df,2p)//B3LYP/6-31G(d) calculations. The calculated relative energies given in kJ mol^{-1} are shown in the parentheses and next to the arrows for the stable species and TSs, respectively. The ZPVE corrections are included.

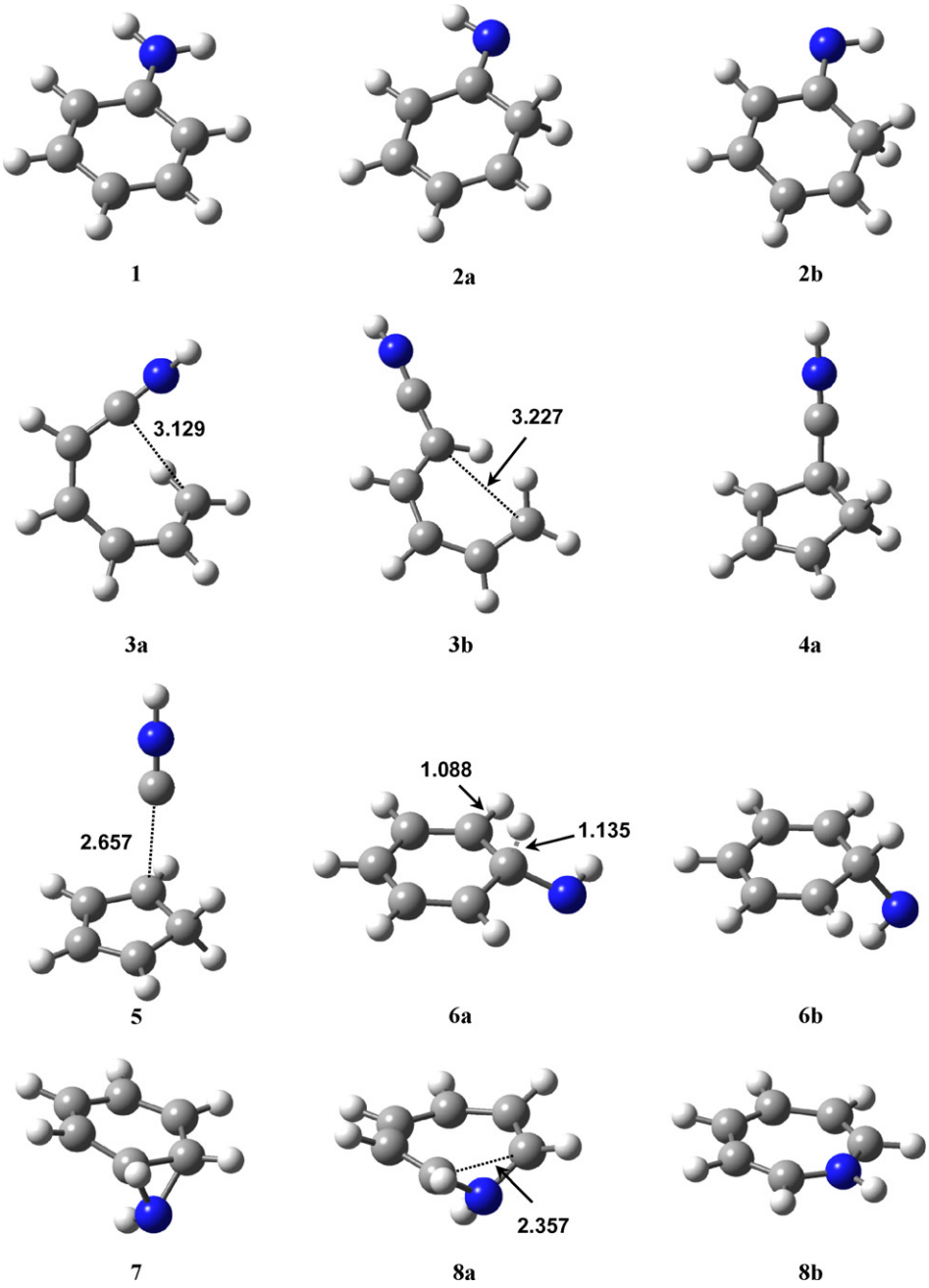

Fig. 1. Geometric structures for selected species optimized using the B3LYP/6-31G(d) calculations. The distances are in Å.

nated 5-cyanocyclopentadiene (PCC^+). PCC^+ was the most unstable among the three $C_6H_6N^+$ ring isomers investigated here. Because the energy needed for the formation of PCC^+ was much higher than that for $CP^{+\bullet}$, it would not be actually observed.

2a or **2b** can be formed from **1** by two consecutive 1,2-H shifts through the intermediate **6a**. Since the energy barrier (329 kJ mol^{-1} for **1** → **6b**) was comparable to that (323 kJ mol^{-1}) for the 1,3-H shift, this pathway can contribute to the dissociation of **1** competitively. On the other hand, the relatively less stable intermediate **6a** can undergo ring expansion, similar with the well-known ring expansion of the toluene molecular ion. A bicyclic isomer **7** can be formed from **6a** through **6b** where the HNCH plane lies vertical to the ring (Fig. 1). When the three-membered ring in **7** is opened by cleavage of the C–C bond, the N atom is inserted into the ring to form the nonplanar 1*H*-azepine ion, **8a**. After isomerization to a more stable planar 1*H*-azepine ion, **8b**, it can either lose $H^\bullet$ to produce the azotropylium ion (ATr^+) or undergo further isomerizations to 2*H*-, 3*H*-, and 4*H*-azepine ions (**8c**, **8d**, and **8e**, respectively) by an H-ring walk. This $H^\bullet$ loss channel is the MERP to produce $C_6H_6N^+$ (Fig. 3). Another $H^\bullet$ loss channel occurs by direct cleavage of a N–H bond to produce the azobenzylium ion (ABz^+).

Comparing with the PES reported previously by Nguyen [22], which was calculated at the B3LYP/6-311++G(d,p) level, the energies of some intermediates such as **2a**, **2b**, **2c**, **4a**, **4b**, and **5** agree within 1 kJmol^{-1}. However, the MERPs to produce $CP^{+\bullet}$ + HNC are different. The MERP of Nguyen contains the pathway **2a** → **2c** → **4b** → **5**, and **2c** → **4b** is the rate-determining step of the MERP with a barrier height 340 kJmol^{-1}. According to the

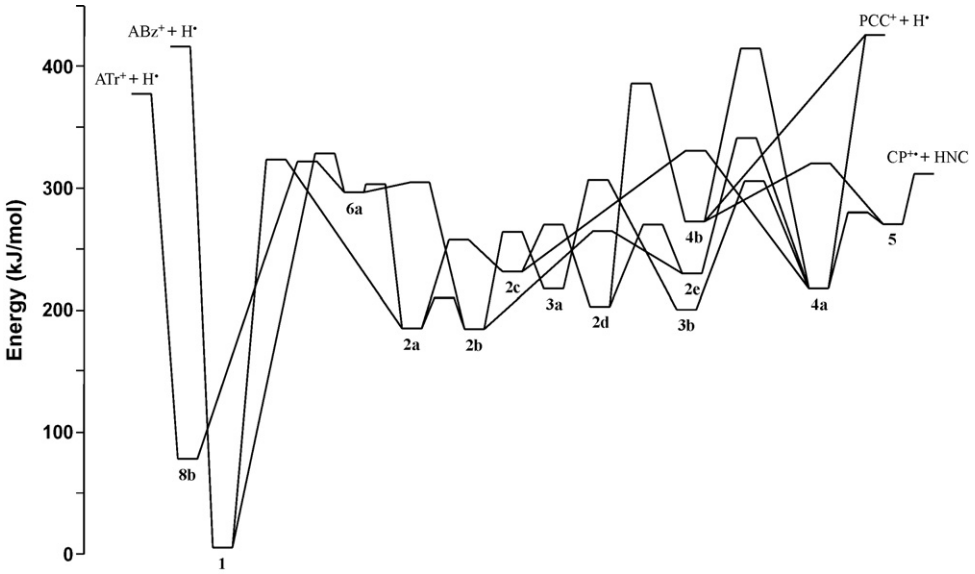

Fig. 2. Potential energy diagram for isomerization and dissociation of the aniline ion, derived from the B3LYP/6-311+G(3df,2p)//B3LYP/6-31G(d) calculations. The pathway to form **8b** from **6a** was approximated by one-well potential for convenience, of which details are shown in Fig. 3.

present result, the pathway **2a** → **2b** → **3a** → **3b** → **4a** → **5** is much more favored (the highest barrier 307 kJmol^{-1}) than suggested by Nguyen, and the rate-determining step is the formation of **2a** from **1**.

3.2. RRKM model calculations

To understand the dissociation kinetics of **1**, we carried out RRKM model calculations using the PES and molecular parameters obtained by DFT calculations. All the pathways described above do not contribute efficiently to the dissociation. Considering the energetics, only the MERP to $CP^{+\bullet}$ + HNC and the pathways through **6a** (Fig. 4) are important in the dissociation at low energy. Therefore, first of all, we assume that the only product ion is $CP^{+\bullet}$ in the dissociation. The H• loss will be considered later.

Since the formation of $CP^{+\bullet}$ occurs by several steps, kinetic analysis was performed using some approximations. The pathways shown in Fig. 4 were approximated as follows:

$$1 \underset{k_{-a}}{\overset{k_a}{\rightleftharpoons}} \mathrm{IG1} \underset{k_{-b}}{\overset{k_b}{\rightleftharpoons}} \mathbf{3b} \xrightarrow{k_c} \mathrm{IG2} \xrightarrow{\text{fast}} CP^{+\bullet} + \mathrm{HNC} \quad (2)$$

where k_i is the rate constant for the i step. IG means an intermediate group in which all the intermediates interconvert rapidly prior to further reactions. IG1 includes **2a**–**2e** and **3a**, and IG2 includes **4a** and **5**. The final dissociation step IG2 (**5**) → $CP^{+\bullet}$ + HNC occurs without a reverse barrier, while the forward and reverse isomerizations between **3b** and IG2 (**4a**) occur via rearrangements with comparable critical energies. Thus, the former occurs much faster because direct bond cleavage is generally more entropically favored than a rearrangement when the critical energies are com-

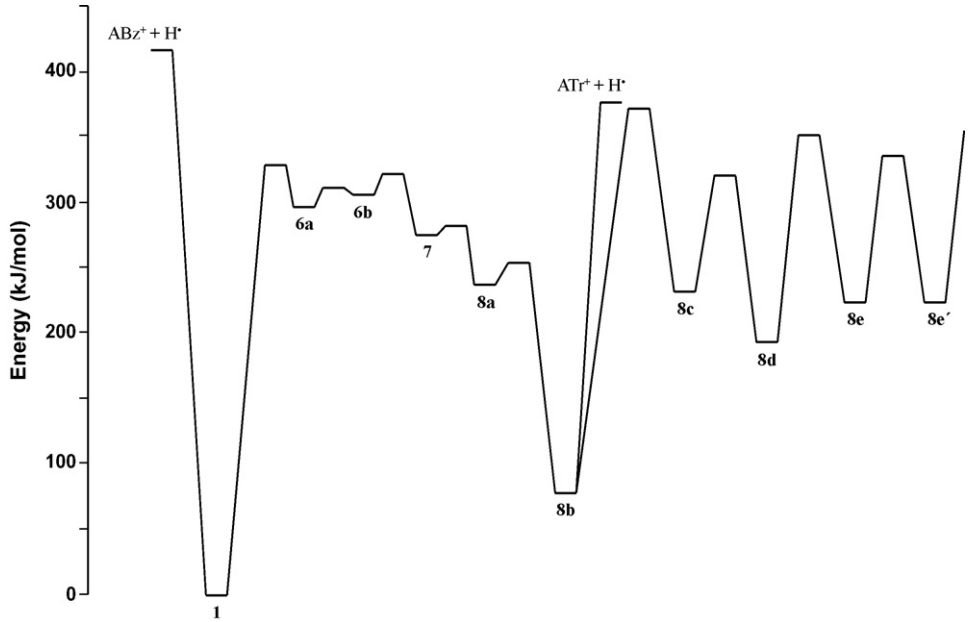

Fig. 3. Potential energy diagram for loss of H• from the aniline ion through ring expansion, derived from the B3LYP/6-311+G(3df,2p)//B3LYP/6-31G(d) calculations.

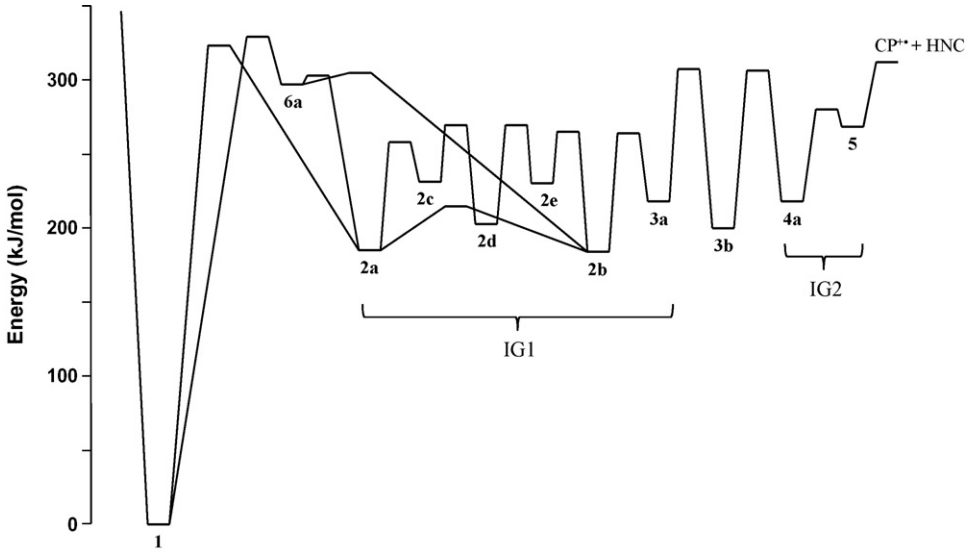

Fig. 4. Potential energy diagram for loss of HNC from the aniline ion, derived from the B3LYP/6-311+G(3df,2p)//B3LYP/6-31G(d) calculations and used for RRKM model calculations.

parable. Therefore, IG2 would dissociate to $CP^{+\bullet}$ rapidly prior to reverse isomerization without affecting the dissociation rate. The time dependences of concentration of **1** and $CP^{+\bullet}$ can be obtained by solving the following rate equations;

$$\frac{d[\mathbf{1}]}{dt} = -k_a[\mathbf{1}] + k_{-a}[\mathrm{IG1}] \quad (3)$$

$$\frac{d[\mathrm{IG1}]}{dt} = k_a[\mathbf{1}] - (k_{-a} + k_b)[\mathrm{IG1}] + k_{-b}[\mathbf{3b}] \quad (4)$$

$$\frac{d[\mathbf{3b}]}{dt} = k_b[\mathrm{IG1}] - (k_{-b} + k_c)[\mathbf{3b}] \quad (5)$$

$$\frac{d[CP^{+\bullet}]}{dt} = k_c[\mathbf{3b}] \quad (6)$$

with the initial condition $[\mathbf{1}] = [\mathbf{1}]_0$ and $[\mathrm{IG1}] = [\mathbf{3b}] = [CP^{+\bullet}] = 0$ at time $t = 0$. All the intermediates were much more unstable than **1**, indicating that their lifetimes are much shorter than **1**. Thus, we can use the steady-state approximation for the intermediates IG1 and **3b**: $d[\mathrm{IG1}]/dt = d[\mathbf{3b}]/dt \cong 0$. With the approximation, we get a solution of the above differential equations as follows;

$$[\mathbf{1}] \cong [\mathbf{1}]_0 \exp(-k_D t) \quad (7)$$

$$[CP^{+\bullet}] \cong \alpha[\mathbf{1}]_0 \left\{1 - \exp(-k_D t)\right\} \quad (8)$$

where α is the constant related to k_i's, and k_D is given by

$$k_D = k_a f \quad (9)$$

Here, f is the fraction of reactions of IG1 toward the dissociation products, expressed as $f = 1 - 1/(1+\beta)$ where $\beta = k_b k_c / \{k_{-a}(k_{-b} + k_c)\}$. The dissociation of **1** and hence the formation of $CP^{+\bullet}$ are characterized by a single rate constant k_D.

The rate constants for the individual steps, k_i's, were calculated by the RRKM formalism [Eq. (1)] using the critical energies and vibrational frequencies obtained from the present DFT calculations. **TS3a_3b**, connecting **3a** and **3b**, was used for calculations of k_b and k_{-b}, and **TS3b_4a** for k_c. As shown in Fig. 4, there are three competitive routes to IG1: **1** → **TS1_2a** → **2a**, **1** → **TS1_6a** → **6a** → **TS6a_2a** → **2a**, and **1** → **TS1_6a** → **6a** → **TS6a_2b** → **2b**. The rate constants of these competitive pathways or reverse ones were summed to obtain k_a or k_{-a}, respectively. In order to calculate rate constants for the latter two routes, the steady-state approximation was used because **6a** was quite unstable. The ratio of contributions to k_a from the channels through **TS1_2a** and **TS1_6a** was 4 at 350 kJ mol^{-1}, decreased with increasing energy up to 500 kJ mol^{-1}, and became a constant 2 at higher energies. Another pathway of **6a**, forming the seven-membered ring isomer (Fig. 3), cannot contribute to the formation of $CP^{+\bullet}$ but can contribute to the dissociation of **1** above the threshold for formation of ATr^+. Its fraction out of the reactions of **6a** was subtracted in the calculation of k_a. However, the fraction was so small as not to affect the dissociation rate constant significantly as described below. In calculation of the density of the states for IG1, the densities of all the intermediates, **2a**–**2e** and **3a**, were summed [10]. The contribution from **3a** was the largest even though it was less stable than **2a** or **2b**. This is due to the open structure of **3a**, making the vibrational frequencies smaller compared to the cyclic isomers. The individual rate constants obtained are shown in Fig. 5. k_a was much smaller than the others, indicating that the intermediates were much less stable than **1** and the steady-state approximation made is valid. The dissociation rate

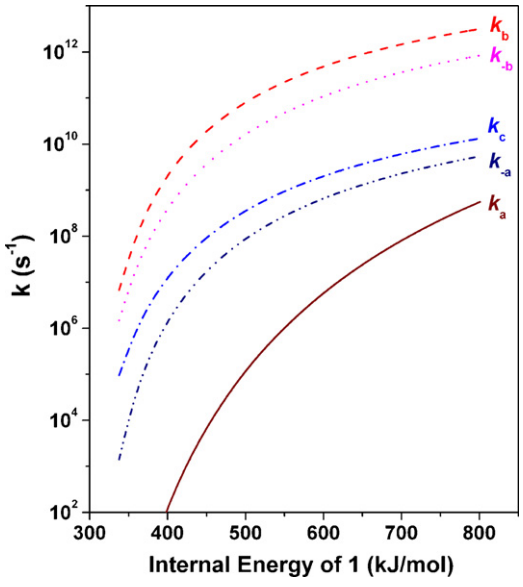

Fig. 5. RRKM rate-energy dependences for the individual reaction steps in Eq. (2).

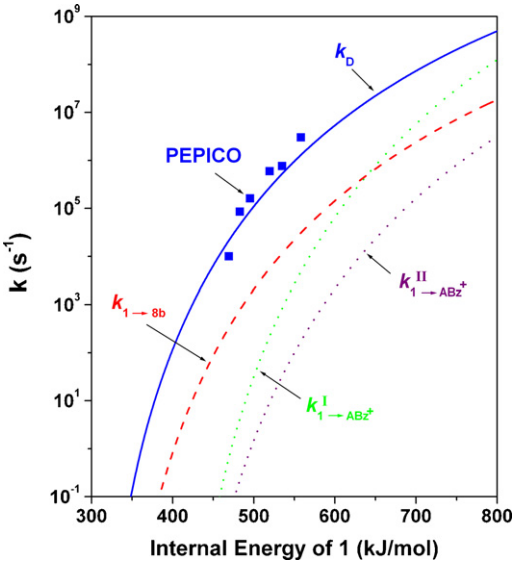

Fig. 6. RRKM rate-energy dependences for k_D, $k_{\mathbf{1}\rightarrow\mathbf{8b}}$, $k^{I}_{1\rightarrow ABz^+}$ and $k^{II}_{1\rightarrow ABz^+}$. The rectangular points are the experimental PEPICO results by Baer and Carney [4]. To convert the photon energy of the PEPICO data to the internal energy, the thermal energy calculated was added.

constant, k_D, estimated by Eq. (9) is shown in Fig. 6, agreeing well with the experimental PEPICO data by Baer and Carney [4] considering experimental error limits and the approximations made here. k_D was somewhat smaller than k_a, and the fraction f decreased with increasing energy. At 400 kJ mol^{-1} f was 0.98 and at 800 kJ mol^{-1}, 0.90. This means that most of **2a** ions formed from **1** would undergo dissociation to CP$^{+\bullet}$.

Lifshitz et al. [2] obtained metastable $C_5H_6^{+\bullet}$ peaks in mass spectra of aniline with a variation of the ion storage time, 1–50 μs. By analyzing the pseudo-Gaussian peak shapes, they suggested that origin of the kinetic energy release (KER) is statistical and not due to a reverse barrier. KER provides information on a final exit channel in consecutive dissociation, while dissociation rate is mainly determined at a rate-determining step. The present result that the final dissociation step had no a reverse barrier supports the suggestion by Lifshitz et al. This leads to the conclusion that the rate of formation of CP$^{+\bullet}$ is mostly determined at the first isomerization steps, through **TS1_2a** or **TS1_6a**, while the KER is determined at the final dissociation step **5** → CP$^{+\bullet}$ + HNC.

As mentioned above, some of **6a** ions formed from **1** can isomerize eventually to **8b** with the rate-determining step **6b** → **7** (Fig. 2). The dissociation through **6a** and **8b** can compete with the CP$^{+\bullet}$ formation above the threshold (377 kJ mol^{-1}) for formation of ATr$^+$. The rate constant ($k_{\mathbf{1}\rightarrow\mathbf{8b}}$) for the formation of **8b** from **1** was calculated using the RRKM formalism, which is shown in Fig. 5. $k_{\mathbf{1}\rightarrow\mathbf{8b}}$ was much smaller than k_D which is actually the rate constant of the formation of CP$^{+\bullet}$. $k_{\mathbf{1}\rightarrow\mathbf{8b}}$ was a small proportion (a few percent) of k_D and increased with increasing energy, up to 4% at 800 kJ mol^{-1}. Below the threshold (416 kJ mol^{-1}) for formation of ABz$^+$, the loss of H$^\bullet$ would occur via **8b** to produce the seven-membered ATr$^+$. Either the steps **1** → **6a** or **8b** → ATr$^+$ + H$^\bullet$ can be the rate-determining step, dependent on the energy. At high energy the rate of the former step would be slower than the latter. Thus, $k_{\mathbf{1}\rightarrow\mathbf{8b}}$ is the higher limit of the rate constant of the formation of ATr$^+$.

Above the threshold for the formation of ABz$^+$ the direct loss of H$^\bullet$ from **1** can compete with the rearrangements leading to formations of CP$^{+\bullet}$ and ATr$^+$, because it was entropically more favored with increasing energy. In order to estimate roughly the rate constant, $k_{1\rightarrow ABz^+}$, of the H$^\bullet$ loss, we carried out RRKM calculations based on activation entropy ($\Delta S^{\ddagger}$) that defines the degree of looseness of the TS [29]. It is well known that RRKM rate constants do not depend on individual vibrational frequencies but on $\Delta S^{\ddagger}$ [10,30]. According to the data compiled by Lifshitz [30] and subsequent work, most of the $\Delta S^{\ddagger}$ values at 1000 K for reactions occurring via a loose TS are in the range 13–46 J mol^{-1} K^{-1} (3–11 eu). Thus, to calculate $k_{1\rightarrow ABz^+}$ the TS frequencies were adjusted for $\Delta S^{\ddagger}_{1000K}$ to become 46 or 13 J mol^{-1} K^{-1} with taking the asymmetric N–H stretching mode for the reaction coordinate. The results are shown in Fig. 6, marked with $k^{I}_{1\rightarrow ABz^+}$ and $k^{II}_{1\rightarrow ABz^+}$, respectively. The actual rate constants would be in between the two rate-energy dependence curves. Up to about 600 kJ mol^{-1}, $k_{1\rightarrow ABz^+}$ was much smaller than k_D. Consequently, because the contributions from both the channels for the H$^\bullet$ loss was negligible up to about 600 kJ mol^{-1}, the above assumption that k_D in Eq. (9) is the dissociation rate constant, actually the rate constant of formation of CP$^{+\bullet}$, is reasonable. However, as the energy increases, the formation of ABz$^+$ would dominate that of ATr$^+$ and compete with the formation of CP$^{+\bullet}$. Then, the overall dissociation rate constant would become larger than k_D because it is sum of the rate constants of the competing dissociation channels.

The good agreement between the RRKM and experimental rate-energy dependences does not mean that the PES obtained is accurate quantitatively because a lot of energies and vibrational frequencies of the $C_6H_7N^{+\bullet}$ species were used in the RRKM calculations. Especially the accuracy of TS frequencies and energies obtained by quantum chemical calculations has not been well evaluated. In this regard, it is worthwhile to investigate the branching ratio of loss of HNC and H$^\bullet$, $[C_5H_6^{+\bullet}]/[C_6H_6N^+]$. The branching ratio estimated from the RRKM rate constants as a function of the energy is shown in Fig. 7. At high energies the branching ratios are in between the two curves, dependant on the looseness of the TS for the ABz$^+$ formation. As the energy increases, the branching ratio decreases. In some of the reported MPI spectra of aniline [3,5], both the $C_5H_6^{+\bullet}$ and $C_6H_6N^+$ peaks appear with much smaller abundance of the latter. In the reported EI spectrum [1] of aniline and CID spectrum [9] of its molecular ion, the $[C_5H_6^{+\bullet}]/[C_6H_6N^+]$ ratios are around 3 and 10, respectively. However, these data cannot be compared with the theoretical prediction shown in Fig. 7 because the energy of the molecular ion is not well defined in

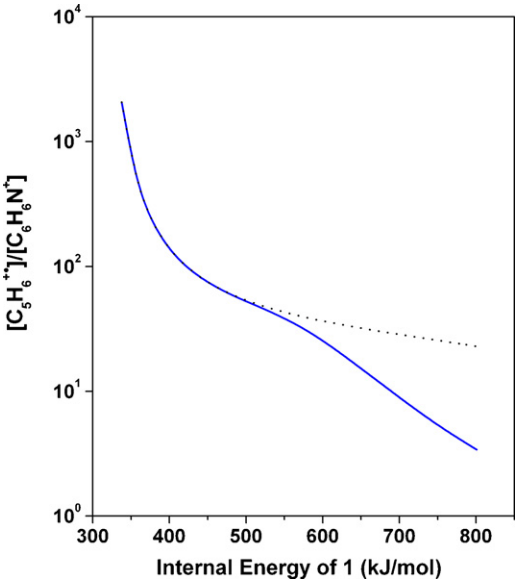

Fig. 7. The $[C_5H_6^{+\bullet}]/[C_6H_6N^+]$ ratio calculated from the RRKM rate-energy dependences shown in Fig. 6. $k_{\mathbf{1}\rightarrow\mathbf{8b}}$ was taken as the rate constant of the formation of ATr$^+$. The solid and dotted lines were calculated using $k^{I}_{1\rightarrow ABz^+}$ and $k^{II}_{1\rightarrow ABz^+}$, respectively.

such experimental observations and the spectra contain fragment ions produced from several consecutive dissociations. On the other hand, the detection of $C_6H_6N^+$ ion has not been mentioned in the reported metastable dissociations [2,4] of the molecular ion having internal energy lower than those prepared by EI, CID, and MPI methods. This experimental trend of the branching ratio on the internal energy agrees with the present theoretical one qualitatively. For the quantitative comparison, further experimental studies are needed to obtain breakdown graph or rate-energy dependence for the energy-selected ions.

Since the H-ring walk in **8b** requires high energy comparable to the H• loss (Fig. 3), the dissociation would occur prior to the H scrambling. Therefore, by means of isotope labeling, the $C_6H_6N^+$ structure cannot be resolved between ATr^+ and ABz^+. In line with this, in an isotope labeling study by EI [1], it was suggested that the lost H• comes from the amino group. The experimental evidence of involvement of the seven-membered ring isomer, the azepine ion, has come from the formation of other product ions. In an MPI study carried out with isotope labeling [3], the involvement of 1*H*-azepine ion was proposed for the formations of CH_2N^+ and $C_3H_3{}^+$. In another isotope labeling study [1], involvement of an intermediate of higher symmetry than **1**, presumably the azepine ion, was suggested for loss of CH_3•.

4. Conclusion

The PES for isomerization and dissociation of **1** was obtained using DFT MO calculations. Ring contraction occurring though the linear isomer (**3a**, **3b**) was more favored than that occurring concertedly from the imidocyclohexadiene isomers (**2c**–**2e**). The formation of $CP^{+\bullet}$ + HNC through the ring contraction via consecutive ring opening and re-closure was the MERP in the dissociation of **1**. Three pathways for loss of H• were found, which produced the five-, six-, and seven-membered ring $C_6H_6N^+$ isomers. From kinetic analysis by RRKM model calculations, previous experimental rate and KER data could be well interpreted. The formation of $CP^{+\bullet}$ was the main dissociation channel, and the formation of ABz^+ and ATr^+ could contribute to the dissociation at high energy.

References

[1] P.N. Rylander, S. Meyerson, E.L. Eliel, J.D. McCollum, J. Am. Chem. Soc. 85 (1963) 2723.
[2] C. Lifshitz, P. Gotchiguian, R. Roller, Chem. Phys. Lett. 95 (1983) 106.
[3] J.A. Zimmerman, R.M. O'Malley, Int. J. Mass Spectrom. Ion Process. 99 (1990) 169.
[4] T. Baer, T.E. Carney, J. Chem. Phys. 76 (1982) 1304.
[5] H. Kühlewind, H.J. Neusser, E.W. Schlag, J. Chem. Phys. 82 (1985) 5452.
[6] D. Proch, D.M. Rider, R.N. Zare, Chem. Phys. Lett. 81 (1981) 430.
[7] O.K. Yoon, W.G. Hwang, J.C. Choe, M.S. Kim, Rapid Commun. Mass Spectrom. 13 (1999) 1515.
[8] J. Watanabe, R. Itakura, A. Hishikawa, K. Yamanouchi, J. Chem. Phys. 116 (2002) 9697.
[9] H.T. Le, R. Flammang, M. Barbieux-Flammang, P. Gerbaux, M.T. Nguyen, Int. J. Mass Spectrom. 217 (2002) 45.
[10] T. Baer, W.L. Hase, Unimolecular Reaction Dynamics: Theory and Experiments, Oxford, New York, 1996.
[11] C. Lifshitz, Y. Gotkis, A. Ioffe, J. Laskin, S. Shaik, Int. J. Mass Spectrom. Ion Process. 125 (1993) 7.
[12] C. Lifshitz, Acc. Chem. Res. 27 (1994) 138.
[13] M.J.S. Dewar, D. Landman, J. Am. Chem. Soc. 99 (1977) 2446.
[14] J.C. Choe, J. Phys. Chem. A 110 (2006) 7655.
[15] J.C. Choe, Chem. Phys. Lett. 435 (2007) 39.
[16] J. Grotemeyer, H.F. Grützmacher, in: A. Macoll (Ed.), Current Topics in Mass Spectrometry and Chemical Kinetics, Heyden, London, 1982, p. 29.
[17] H.F. Grützmacher, N. Harting, Eur. J. Mass Spectrom. 9 (2003) 327.
[18] D. Norberg, P.-E. Larsson, N. Salhi-Benachenhou, J. Phys. Chem. A 112 (2008) 4694.
[19] J.C. Choe, J. Phys. Chem. A (2008).
[20] J.C. Choe, Int. J. Mass Spectrom. 237 (2004) 1.
[21] J.C. Choe, Int. J. Mass Spectrom. 242 (2005) 5.
[22] M.T. Nguyen, in: Z. Rappoport (Ed.), The Chemistry of Anilines, Wiley, New York, 2007.
[23] H.T. Le, R. Flammang, P. Gerbaux, G. Bouchoux, M.T. Nguyen, J. Phys. Chem. A 105 (2001) 11582.
[24] F. Muntean, P.B. Armentrout, J. Phys. Chem. B 106 (2002) 8117.
[25] M.J. Frisch, G.W. Trucks, H.B. Schlegel, G.E. Scuseria, M.A. Robb, J.R. Cheeseman, J.A. Montgomery Jr., T. Vreven, K.N. Kudin, J.C. Burant, J.M. Millam, S.S. Iyengar, J. Tomasi, V. Barone, B. Mennucci, M. Cossi, G. Scalmani, N. Rega, G.A. Petersson, H. Nakatsuji, M. Hada, M. Ehara, K. Toyota, R. Fukuda, J. Hasegawa, M. Ishida, T. Nakajima, Y. Honda, O. Kitao, H. Nakai, M. Klene, X. Li, J.E. Knox, H.P. Hratchian, J.B. Cross, V. Bakken, C. Adamo, J. Jaramillo, R. Gomperts, R.E. Stratmann, O. Yazyev, A.J. Austin, R. Cammi, C. Pomelli, J.W. Ochterski, P.Y. Ayala, K. Morokuma, G.A. Voth, P. Salvador, J.J. Dannenberg, V.G. Zakrzewski, S. Dapprich, A.D. Daniels, M.C. Strain, O. Farkas, D.K. Malick, A.D. Rabuck, K. Raghavachari, J.B. Foresman, J.V. Ortiz, Q. Cui, A.G. Baboul, S. Clifford, J. Cioslowski, B.B. Stefanov, G. Liu, A. Liashenko, P. Piskorz, I. Komaromi, R.L. Martin, D.J. Fox, T. Keith, M.A. Al-Laham, C.Y. Peng, A. Nanayakkara, M. Challacombe, P.M.W. Gill, B. Johnson, W. Chen, M.W. Wong, C. Gonzalez, J.A. Pople, Gaussian 03, Revision C. 02, Gaussian, Inc., Wallingford, CT, 2004.
[26] M.W. Wong, L. Radom, J. Phys. Chem. A 102 (1998) 2237.
[27] A.P. Scott, L. Radom, J. Phys. Chem. A 100 (1996) 16502.
[28] T. Beyer, D.R. Swinehart, ACM Commun. 16 (1973) 379.
[29] Even though the activation entropy is defined for a canonical ensemble, it is often used to obtain a quantitative measure of the degree of looseness of the transition state in analysis for a microcanonical ensemble. See page 217 of Ref. [10] for the details.
[30] C. Lifshitz, Adv. Mass Spectrom. 11 (1989) 713.